IOPscience iopscience.iop.org

Home Search Collections Journals About Contact us My IOPscience

The effect of the interface oxidation on tunneling conductance of $Co_2MnSi/MgO/Co_2MnSi$ magnetic tunnel junction

This article has been downloaded from IOPscience. Please scroll down to see the full text article.

2009 J. Phys.: Condens. Matter 21 064245

(http://iopscience.iop.org/0953-8984/21/6/064245)

View the table of contents for this issue, or go to the journal homepage for more

Download details:
IP Address: 129.252.86.83
The article was downloaded on 29/05/2010 at 17:49

Please note that terms and conditions apply.

J. Phys.: Condens. Matter **21** (2009) 064245 (6pp) doi:10.1088/0953-8984/21/6/064245

The effect of the interface oxidation on tunneling conductance of $Co_2MnSi/MgO/Co_2MnSi$ magnetic tunnel junction

Yoshio Miura, Kazutaka Abe and Masafumi Shirai

Research Institute of Electrical Communication, Tohoku University, Katahira 2-1-1, Aoba-ku, Sendai 980-8577, Japan

Received 20 July 2008, in final form 11 November 2008
Published 20 January 2009
Online at stacks.iop.org/JPhysCM/21/064245

Abstract
We investigate and discuss the effects of interfacial oxidation on electronic structures and tunnel conductance of the $Co_2MnSi/MgO/Co_2MnSi(001)$ magnetic tunnel junction (MTJ) on the basis of first-principles calculations. It is found that the MnSi termination tends to be oxidized compared with the Co termination because of the relaxation of atomic positions in the MnSi-terminated interface. Furthermore, we found that the single oxide layer inserted on both sides of the junction greatly decreases the tunnel conductance of the MTJ in parallel magnetization. We concluded that the relaxation of the Mn atomic position in the oxidized junction reduces the coupling of the Δ_1 states between the Co_2MnSi electrode and the MgO barrier and causes significant interfacial scattering of the majority-spin electrons with Δ_1 symmetry at the oxidized layer.

(Some figures in this article are in colour only in the electronic version)

1. Introduction

The tunneling magnetoresistance (TMR) [1–3] of magnetic tunnel junctions (MTJs) consisting of ferromagnet/insulator/ferromagnet sandwiches has attracted strong scientific interest, owing to their potential application in spintronics, such as magnetoresistive random access memory (MRAM) and the read-out head of hard disk drives. Recently, Butler *et al* predicted a TMR ratio as high as 6000% for the Fe/MgO/Fe(001) MTJ using the first-principles layer–KKR method [4]. They found that the decay of the tunneling wavefunction of Δ_1 states is very slow compared with that of Δ_2 and Δ_5 states in the MgO barrier. Furthermore, bcc-Fe is half-metallic on the Δ_1 band, providing a very large TMR in the Fe/MgO/Fe(001) MTJ. This theory has been confirmed by several experimental groups and a much larger TMR was obtained at room temperature (RT) [5, 6]. In addition, the TMR ratio was increased to 500% at RT for the MTJ with CoFeB electrodes and MgO barrier [7].

While the Fe/MgO/Fe(001) MTJ and related systems is applied to the MRAM, lower resistance is required for the TMR devices to achieve ultra-high speed and high density in future spintronics applications. To this end, one needs a tunneling junction with a thin MgO barrier. However, the TMR of Fe/MgO/Fe(001) and related systems rapidly decreases with decreasing MgO barrier thickness, owing to the contribution of the minority-spin Δ_5 and Δ_2 states to the tunneling conductance through a thin MgO barrier. Half-metallic ferromagnets (HMFs) [8], which show complete (100%) spin polarization at the Fermi level, are expected to overcome this problem, because the MTJ with half-metallic electrodes and MgO barrier (HMF/MgO/HMF) can suppress the tunneling from the minority-spin Δ_5 and Δ_2 states in such a thin MgO barrier. Recently, MgO-based MTJs with Co-based full-Heusler alloy electrodes ($Co_2Fe(Al, Si)$, $Co_2(Cr, Fe)Al$ and Co_2MnSi) have been fabricated, and the TMR has steadily improved [9–11].

In MTJs, electronic and magnetic properties of the interfacial region of ferromagnetic electrodes with an insulating barrier play an important role in the spin-dependent tunneling characteristics. In particular, oxidation of ferromagnetic electrodes near interfaces degrades the

 © 2009 IOP Publishing Ltd Printed in the UK

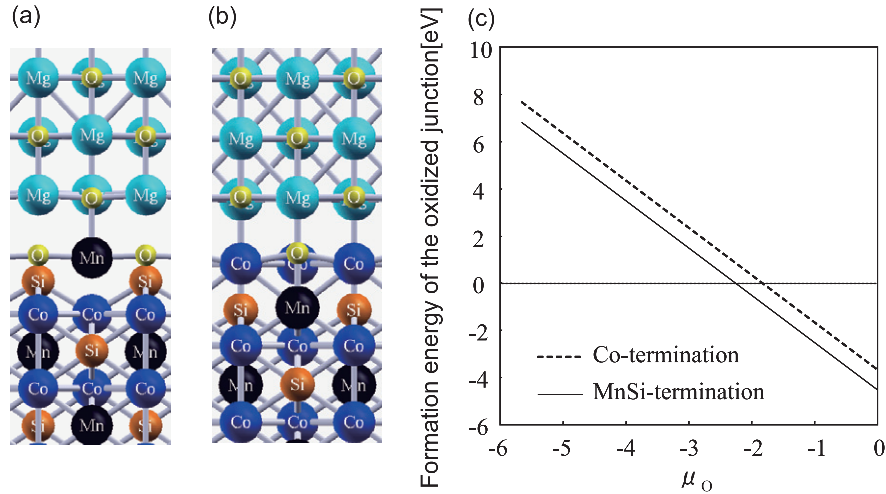

Figure 1. Magnification of the cross-sectional view of the $Co_2MnSi/MgO(001)$ interfacial structures with a single oxide layer after relaxation of the atomic positions for (a) Co- and (b) MnSi-terminated $Co_2MnSi/MgO(001)$ interface. (c) The formation energy of the oxidized $Co_2MnSi/MgO(001)$ junctions for the MnSi termination (solid line) and the Co termination (dashed line) as a function of μ_O within the thermodynamically allowed range $\mu_{MgO} - \mu_{Mg(hcp)} \leqslant \mu_O \leqslant \mu_{O_2}$ (see the text).

efficiency of TMR devices. For example, first-principles calculation results of the Fe/MgO/Fe MTJ [12] show that a single layer of iron oxide at the interface between the Fe electrode and the MgO barrier greatly reduces the tunneling conductance and the TMR owing to reduction of the coupling of the Δ_1 state of the Fe layer to the MgO layer. Since the Co-based full-Heusler alloys such as Co_2MnSi also have the Δ_1 band around the Fermi level in the majority-spin state [13], the presence of Mn-oxide and Co-oxide layers between the Co_2MnSi electrode and the MgO barrier will degrade the coherent tunneling through the Δ_1 channel of the MTJ in parallel magnetization. In this work, we theoretically investigate the effects of oxidation in the $Co_2MnSi/MgO(001)$ junction on the electronic and transport properties of the MTJ by using first-principles electronic structure calculations and conductance calculations [15].

2. Computational details

We perform first-principles calculations for supercells consisting of Co_2MnSi and MgO, using the density functional theory within the generalized-gradient approximation for the exchange–correlation energy [16]. We adopt plane-wave basis sets along with the ultra-soft pseudopotential method by using the quantum code ESPRESSO [15]. The number of **k** points is taken to be $10 \times 10 \times 1$ for all cases, and Methfessel–Paxton smearing with a broadening parameter of 0.01 Ryd is used. The cutoff energy for the wavefunction and charge density is set to 30 Ryd and 300 Ryd, respectively.

For conductance calculations, we consider an open quantum system consisting of a scattering region corresponding to MgO and a junction with Co_2MnSi attached to left and right semi-infinite electrodes corresponding to bulk Co_2MnSi [13, 14]. The potential in the scattering equation can be obtained from the self-consistent electronic structure calculations for the supercell containing a left and a scattering region. Since our system is repeated periodically in the xy plane and propagating states can be assigned by an in-plane wavevector $k_\parallel = (k_x, k_y)$ index, different $k_\parallel$ do not mix and can be treated separately. Furthermore, our approach neglects the spin–orbit interaction and noncollinear spin configuration. We solve scattering equations for some fixed $k_\parallel$ and spin index on the basis of Choi and Ihm's approach [17, 18].

3. Results and discussions

Our $Co_2MnSi/MgO/Co_2MnSi(001)$ MTJ is constructed in a tetragonal supercell, where the in-plane lattice parameter of the supercell is fixed at 3.99 Å. These values correspond to $a_0/\sqrt{2}$, where a_0 is the lattice constant of the bulk Co_2MnSi (5.65 Å). The lattice mismatches between Co_2MnSi and MgO on the 45° in-plane rotation at the (001) face are 5.1%. The $Co_2MnSi/MgO(001)$ interface has two types of termination on Co_2MnSi, namely the Co termination and the MnSi termination. We prepare the supercell from multilayers containing nine atomic layers of MgO and 17 and 15 atomic layers of Co_2MnSi for the Co- and MnSi-terminated interfaces, respectively.

First, we minimized the total energy of the supercell by relaxing interfacial atomic positions by changing the longitudinal size of the supercell in order to determine the stable configuration for each termination in $Co_2MnSi/MgO(001)$ junctions. We obtained the O-top configuration where atoms terminating Co_2MnSi are positioned on top of the O atoms of the MgO(001) surface. The interfacial Co–O distance in the Co termination is rather small ∼2.00 Å for the $Co_2MnSi/MgO(001)$ junctions. On the other hand, the interfacial Mn–O and Si–O distances in the MnSi termination are 2.25 Å and 3.17 Å, respectively. We consider that the difference in the covalent bond radius of the Mn (1.39 Å) atom and Si (1.11 Å) atom causes different interfacial distances of Mn–O and Si–O in the MnSi termination [14].

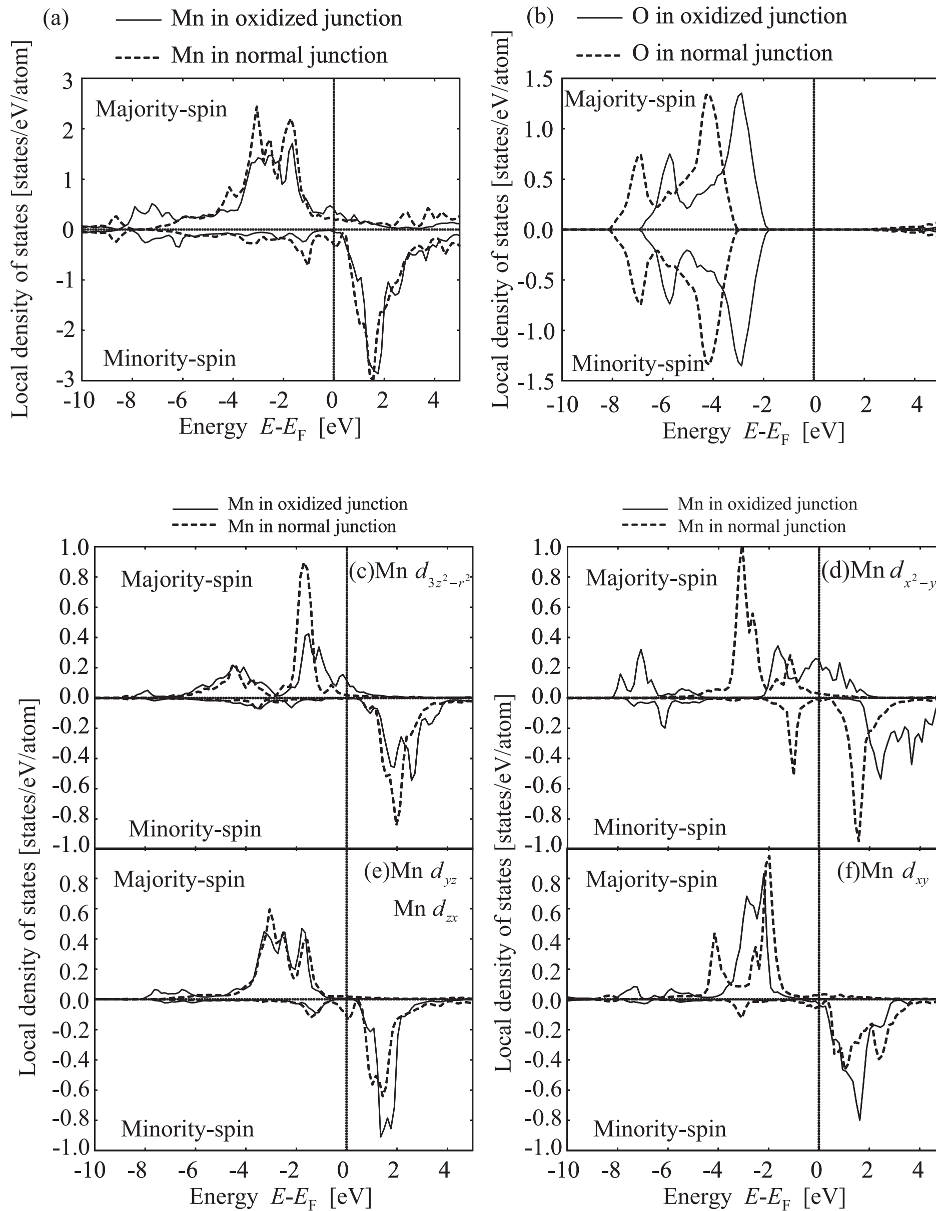

Figure 2. The local density of states (LDOS) of interfacial (a) Mn (total), (b) O in the interior region (total), (c) Mn $3d_{3z^2-r^2}$, (d) Mn $3d_{3x^2-y^2}$, (e) Mn $3d_{yz}$ or $3d_{zx}$, and (f) Mn $3d_{xy}$ in the oxidized $Co_2MnSi/MgO(001)$ junction as a function of energy relative to the Fermi energy. The LDOS in the normal (non-oxidized) junction is also shown for reference by a dashed line in each figure. The sign of LDOS indicates the majority-spin (positive) and minority-spin (negative) states.

Then, we put two oxygen atoms between the Co_2MnSi electrode and the MgO barrier on top of the Mg atoms in order to form a single oxide layer on both sides of the junction, and minimize the total energy of the supercell by relaxing interfacial atomic positions. Figure 1 shows the cross-sectional view of the oxidized $Co_2MnSi/MgO(001)$ junctions after relaxation of atomic positions for (a) MnSi and (b) Co terminations. In order to compare the stability of the single oxide layer for each termination, we calculate the formation energy of the oxidized junction defined by

$$E_{\mathrm{form}}^{\mathrm{oxide}} = E_{\mathrm{tot}}^{\mathrm{oxide}} - E_{\mathrm{tot}}^{\mathrm{normal}} - N_{\mathrm{O}}\mu_{\mathrm{O}} \qquad (1)$$

where $E_{\mathrm{tot}}^{\mathrm{oxide}}(E_{\mathrm{tot}}^{\mathrm{normal}})$ are the total energy of the supercell with (without) a single oxide layer for each termination, N_{O} is the difference in the number of oxygen atoms between the oxidized junction and the normal junction and μ_{O} is the chemical potential of the oxygen atom. Since the supercell with the oxidized junction is non-stoichiometric only on O atoms as compared to the supercell of the normal junction, the $E_{\mathrm{form}}^{\mathrm{oxide}}$ can be expressed as a function of μ_{O} only. In addition, the chemical potential of the constituent atoms in the thermodynamic equilibrium condition cannot exceed the corresponding one of the elemental phase, i.e. the upper limit of μ_{O} can be derived from the total energy of an oxygen molecule per atom (μ_{O_2}). Furthermore, assuming the thermodynamic equilibrium condition on MgO, i.e. $\mu_{\mathrm{MgO}} = \mu_{\mathrm{Mg}} + \mu_{\mathrm{O}}$ and taking μ_{MgO} from the bulk structure, we can determine the lower limit of μ_{O} as $\mu_{\mathrm{O}} \geqslant \mu_{\mathrm{MgO}} - \mu_{\mathrm{Mg}}$.

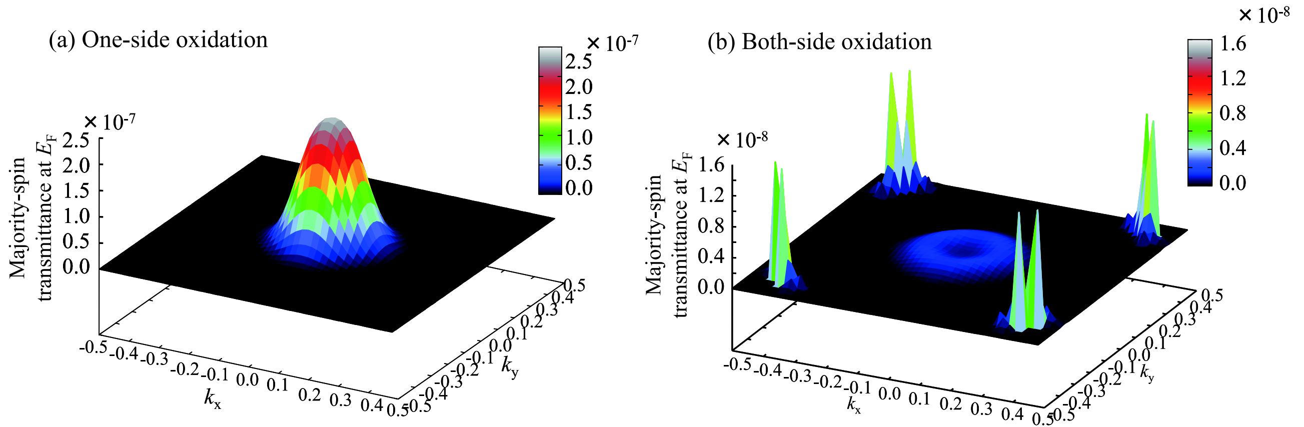

Figure 3. In-plane wavevector $k_\parallel = (k_x, k_y)$ dependence of majority-spin transmittance at the Fermi level for (a) Co_2MnSi/O/MgO(9)/Co_2MnSi(001) MTJ (one-side oxidation), (b) Co_2MnSi/O/MgO(9)/O/Co_2MnSi(001) MTJ (both-sides oxidation) in parallel magnetization.

Here, the upper limit of μ_{Mg} is again derived from the total energy of the bulk hcp structure ($\mu_{Mg(hcp)}$). Thus, the E_{form}^{oxide} is expressed within the thermodynamically allowed range $\mu_{MgO} - \mu_{Mg(hcp)} \leqslant \mu_O \leqslant \mu_{O_2}$.

In figure 1(c), we report the calculated formation energy of the oxidized junction for the MnSi and Co terminations as a function of μ_O. The negative value of E_{form}^{oxide} indicates that the Co_2MnSi/MgO(001) junction is oxidized at the given μ_O, which is relevant to the oxygen atom content of the system. As can be seen in figure 1(c), the E_{form}^{oxide} shows negative values in the high μ_O region. This means that control of the oxygen atom content will be required during fabrication of the Co_2MnSi/MgO(001) junction. Furthermore, E_{form}^{oxide} of the MnSi termination is smaller than that of the Co termination, indicating that the MnSi-terminated interface is easy to be oxidized compared with the Co-terminated interface. Because the MnSi termination has a large interstitial region owing to the relaxation of Si atomic position into the Co atom side, the MnSi-terminated interface easily incorporates oxygen atoms. On the other hand, the Co-terminated interface has strong bonding with MgO, and the incorporation of oxygen atoms involves energy loss as compared to the MnSi termination. This suggests that we can control interfacial oxidation in the Co_2MnSi/MgO(001) junction by modulating its termination.

Figure 2(a) shows the majority- and minority-spin local density of states (LDOS) of the interfacial Mn atom in the oxidized junction (solid line) as a function of energy relative to the Fermi energy. The LDOS of the interfacial Mn atom in the normal junction (dashed line) are shown for reference. We can find in figure 2(a) that the overall shape of the LDOS of the interfacial Mn atom hardly changes after oxidation. The local charge around the interfacial Mn atom within the covalent bond radius (1.39 Å) is about 6.0 in the oxidized junction, while it is about 6.3 in bulk Co_2MnSi. Furthermore, the local moments of the interfacial Mn are $4.06\mu_B$ at the normal junction and $3.99\mu_B$ at the oxidized junction, which are both increased from the local moment of Mn ($3.31\mu_B$) in bulk Co_2MnSi. These results indicate that a single layer of oxidation does not significantly affect the electronic configuration of the interfacial Mn atom compared to the normal junction as a result of the charge screening effect from the Co_2MnSi electrode. We consider that several layers of oxidation will be necessary to obtain an electronic configuration appearing in the bulk Mn oxide.

Then, we present in figures 2(c)–(f) the majority- and minority-spin LDOS projected to each Mn 3d orbital in the oxidized junction (solid line) as a function of energy relative to the Fermi energy. The corresponding LDOS in the normal junction (dashed line) is shown for reference. It is found that effects of the single oxide layer are significant in the LDOS of Mn $3d_{3z^2-r^2}$, $3d_{x^2-y^2}$ and $3d_{xy}$. Since additional oxygen atoms are positioned in the same xy plane with the interfacial Mn atom (see figure 1(a)), Mn $3d_{x^2-y^2}$ and $3d_{xy}$ hybridize with O $2p_x$ and $2p_y$, leading to changes in the LDOS of Mn $3d_{x^2-y^2}$ and $3d_{xy}$ in the oxidized junction. Furthermore, we can find in figure 2(d) a characteristic reduction of the LDOS peak at $E - E_F \sim -0.8$ eV for Mn $3d_{3z^2-r^2}$ in the oxidized junction compared to those in the normal junction. This can be attributed to the relaxation of the interfacial Mn atom in the oxidized junction, where the Mn atom moves away from the subinterfacial Co atoms (see figure 1(a)). In fact, the interfacial Co–Mn distance in the oxidized junction is increased to 2.91 Å compared to that in the normal junction (2.58 Å). This atomic relaxation weakens the bonding between the interfacial Mn and subinterfacial Co atoms, and reduces the LDOS peaks in the Mn $3d_{3z^2-r^2}$ at the corresponding energy. Since the $3d_{3z^2-r^2}$ orbital has the Δ_1 symmetry, the change of the Mn $3d_{3z^2-r^2}$ wavefunction at the oxidized junction will influence the coherent tunneling through the Δ_1 channel of the MTJ. We confirmed that the majority-spin Δ_1 band around the Fermi level is mainly composed of Mn-$3d_{3z^2-r^2}$ and Si-s.

To look at how the single oxide layer at the Co_2MnSi/MgO (001) junction affects the transport properties of the MTJ, we calculate the tunneling conductance of the Co_2MnSi/O/MgO/Co_2MnSi(001) MTJ (one-side oxidation) and the Co_2MnSi/O/MgO/O/Co_2MnSi(001) MTJ (both-sides oxidation) at the Fermi level in parallel magnetization. Figures 3(a) and (b) plot the majority-spin transmittance for

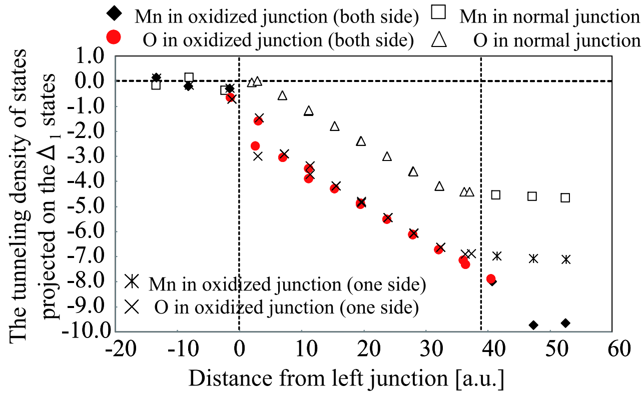

Figure 4. The majority-spin tunneling density of states projected on the Δ_1 states at the Fermi level as a function of the distance from the left $Co_2MnSi/MgO(001)$ interface for the normal junction (open triangle and square), the junction with one-side oxidation ($\times$ and $*$) and the junction with both-sides oxidation (filled circle and diamond) in parallel magnetization. The scale of the vertical axis is logarithmic.

the oxidized MTJ as a function of the in-plane wavevector $k_\parallel = (k_x, k_y)$. As can be seen in figure 3(a), the $k_\parallel$ dependence of transmittance for one-side oxidation has a broad peak centered at $k_\parallel = (0, 0)$ owing to the coherent tunneling through the Δ_1 channel, which is similar to that of the normal junction, i.e. $Co_2MnSi/MgO/Co_2MnSi(001)$ MTJ [14]. On the other hand, the $k_\parallel$ dependence of transmittance for both-sides oxidation has no peak at $k_\parallel = (0, 0)$ and shows spiky structures in the two-dimensional (2D) Brillouin zone, which were the so-called *hot spot* conductance and attributed to the resonant tunneling between the interface states [19]. These results indicate that one-side oxidation does not change the $k_\parallel$ dependence of transmittance, while both-sides oxidation significantly reduces the tunneling conductance through Δ_1.

The averaged conductance over the 2D Brillouin zone for the MTJ with an oxidized junction is about $1.02 \times 10^{-10} G_0$ for one-side oxidation and $2.67 \times 10^{-10} G_0$ for both-sides oxidation, which are smaller than $1.54 \times 10^{-6} G_0$ for the MTJ with the normal junction, where G_0 is in e^2/h units. It is pointed out by Belashchenko *et al* and Velev *et al* that an asymmetric junction reduces the tunneling conductance compared with the symmetric one because the resonant tunneling occurs only at the two identical interfaces [20–22]. In our results, the resonant tunneling is suppressed in the junction with one-side (asymmetric) oxidation. However, the coherent tunneling through the Δ_1 channel is still effective, producing a larger conductance compared with both-sides (symmetric) oxidation.

To confirm the behaviors of the tunneling wavefunction in the MTJ with the oxidized junction, we calculate the projected density of states of the tunneling wavefunction (TDOS) on the Δ_1 states. Figure 4 shows the majority-spin TDOS at the Fermi level as a function of the distance from the left $Co_2MnSi/MgO(001)$ junction for the MTJ in parallel magnetization. We can find an abrupt drop of the TDOS at the oxidized junction, leading to two orders of magnitude smaller TDOS compared with that of the normal junction in the interior region of the MgO barrier. It is clear evidence of significant interfacial scattering of the majority-spin electrons with Δ_1 symmetry at the oxidized $Co_2MnSi/MgO(001)$ interface. The decay rate of the TDOS in the interior region of the MgO barrier is almost the same for both the oxidized junction and the normal junction. This means that very small conductance in the oxidized junction can be attributed mainly to reduced coupling of the Δ_1 states of the Co_2MnSi electrode to the MgO barrier at the interface. The TDOS of the junction with both-sides oxidation again drops by two orders of magnitude, which acts to disturb the coherent tunneling through the Δ_1 channel. We consider that the relaxation of the interfacial Mn atom in the oxidized junction is a main contributing factor of the reduction of the coupling of the Δ_1 sates.

Another possible mechanism for the reduction of the tunneling conductance is due to elimination of states around the gamma point by interface states and the creation of an additional tunneling barrier for the states with small values of the transverse momenta [23, 24]. In figure 2(b), we show the LDOS of O atoms in the interior region of the MgO barrier and estimate the tunneling barrier height V_{barrier} from the conduction band bottom of the LDOS of interior O atoms. We obtain about $V_{\mathrm{barrier}} \approx 3.0$ eV for the oxidized junction (both-sides oxidation) and $V_{\mathrm{barrier}} \approx 2.0$ eV for the normal junction. In the free-electron model, the barrier height contributes to the decay of the wavefunction at the barrier region with a $\sim \sqrt(V_{\mathrm{barrier}})$ factor for all states. We consider that the increase of the tunneling barrier in the oxidized junction also contributes to the reduction of the tunneling conductance especially for states with $k_\parallel \neq 0$.

Finally, we discuss the effects of oxidation on the TMR ratio of the MTJ. In our calculations, the spin-flip process is not included and the minority-spin transmittance at the Fermi energy becomes zero owing to the half-metallic character of bulk Co_2MnSi. This leads to totally zero transmittance at the Fermi energy for the MTJ with anti-parallel magnetization. However, as is discussed by Popescu *et al* and Chantis *et al*, the spin-flip process through the spin–orbit coupling affects the tunneling conductance of the MTJ [25, 26]. Furthermore, Mavropoulos, *et al* pointed out that spin-flip processes such as magnon excitations and inelastic scattering through interface states produce the tunneling conductance in the anti-parallel magnetization at RT [27]. We consider that the oxidation of the MTJ has two factors in the reduction of the TMR ratio. One is the decrease of tunneling conductance in parallel magnetization (see figure 4), while the other is the increase of the tunneling conductance in anti-parallel magnetization. Our results show that LDOSs of the oxidized junction have additional states in the minority-spin gap. This would contribute to the tunneling conductance if the spin-flip processes at the interface are included.

4. Summary

We have investigated effects of interface oxidation in the $Co_2MnSi/MgO(001)$ junction on the electronic structure and the tunnel conductance of the MTJ on the basis of first-principles calculations. We found that the MnSi-terminated

interface is easy to be oxidized compared with the Co-terminated interface because of the relaxation of atomic positions in the MnSi-terminated interface. The overall shape of the LDOS of the interfacial Mn atom hardly changes after oxidation, indicating that a single layer of oxidation does not significantly affect the electronic configuration of the interfacial Mn atom compared with the normal junction as a result of the charge screening effect from the Co_2MnSi electrode. It is considered that several layers of oxidation will be necessary to obtain an electronic configuration appearing in the bulk Mn oxide. The transmittance of the MTJ with one-side oxidation shows a coherent tunneling through the Δ_1 channel, indicating that one-side oxidation does not significantly affect the transport properties of the MTJ. However, both-sides oxidation produces the resonant tunneling and considerably decreases the tunnel conductance of the MTJ in parallel magnetization. These results indicate that suppression of both-sides oxidation at the MTJ is crucial in the Co_2MnSi/MgO/Co_2MnSi(001) MTJ.

Acknowledgments

This work was supported in part by a Grant-in-Aid for Scientific Research in Priority Areas, 'Creation and Control of Spin Current' (no. 19048002) and 'Development of New Quantum Simulators and Design' (no. 17064001), and by 'High-Performance Low-Power Consumption Spin Devices and Storage Systems' program under Research and Development for Next-Generation Information Technology by MEXT.

References

[1] Miyazaki T and Tezuka N 1995 *J. Magn. Magn. Mater.* **139** L231
[2] Moodera J S, Kinder L R, Wong T M and Meservey R 1995 *Phys. Rev. Lett.* **74** 3273
[3] Zhu J-G and Park C 2006 *Mater. Today* **9** 36–45
[4] Butler W H, Zhang X-G and Schulthess T C 2001 *Phys. Rev.* B **63** 054416
[5] Parkin S S P, Kaiser C, Panchula A, Rice P M, Hughes B, Samant M and Yang S-H 2004 *Nat. Mater.* **3** 862
[6] Yuasa S, Nagahama T, Fukushima A, Suzuki Y and Ando K 2004 *Nat. Mater.* **3** 868
[7] Ikeda S, Hayakawa J, Lee Y M, Matsukura F, Ohno Y, Hanyu T and Ohno H 2007 *IEEE Trans. Electron Devices* **54** 991
[8] de Groot R A, Mueller F M, van Engen P G and Buschow K H J 1983 *Phys. Rev. Lett.* **50** 2024
[9] Tezuka N, Ikeda N, Sugimoto S and Inomata K 2006 *Appl. Phys. Lett.* **89** 252508
[10] Marukame T and Yamamoto M 2007 *J. Appl. Phys.* **101** 083906
[11] Ishikawa T, Hakamata S, Matsuda K-i, Uemura T and Yamamoto M 2008 *J. Appl. Phys.* **103** 07A919
[12] Zhang X-G, Butler W H and Bandyopadhyay A 2003 *Phys. Rev.* B **68** 092402
[13] Miura Y, Uchida H, Oba Y, Nagao K and Shirai M 2007 *J. Phys.: Condens. Matter* **19** 365228
[14] Miura Y, Uchida H, Oba Y, Abe K and Shirai M 2008 *Phys. Rev.* B **78** 064416
[15] Baroni S, Dal Corso A, de Gironcoli S and Giannozzi P http://www.pwscf.org
[16] Perdew J P, Burke K and Ernzerhof M 1996 *Phys. Rev. Lett.* **77** 3865
[17] Choi H J and Ihm J 1999 *Phys. Rev.* B **59** 2267
[18] Smogunov A, Dal Corso A and Tosatti E 2004 *Phys. Rev.* B **70** 045417
[19] Wunnicke O, Papanikolaou N, Zeller R, Dederichs P H, Drchal V and Kudrnovsky J 2002 *Phys. Rev.* B **65** 064425
[20] Tusche C, Meyerheim H L, Jedrecy N, Renaud G, Ernst A, Henk J, Bruno P and Kirschner J 2005 *Phys. Rev. Lett.* **95** 176101
[21] Velev J P, Belashchenko K D and Tsymbal E Y 2006 *Phys. Rev. Lett.* **96** 119601
[22] Tusche C, Meyerheim H L, Jedrecy N, Renaud G, Ernst A, Henk J, Bruno P and Kirschner J 2006 *Phys. Rev. Lett.* **96** 119602
[23] Belashchenko K D, Tsymbal E Y, van Schilfgaarde M, Stewart D A, Oleynik I I and Jaswal S S 2004 *Phys. Rev.* B **69** 174408
[24] Belashchenko K D, Velev J P and Tsymbal E Y 2005 *Phys. Rev.* B **72** 140404(R)
[25] Popescu V, Ebert H, Papanikolaou N, Zeller R and Dederichs P 2004 *J. Phys.: Condens. Matter* **16** S5579
[26] Chantis A N, Belashchenko K D, Tsymbal E Y and van Schilfgaarde M 2007 *Phys. Rev. Lett.* **98** 046601
[27] Mavropoulos P, Lezaic M and Blügel S 2005 *Phys. Rev.* B **72** 174428